EasyChair Preprint

№ 10619

Enhancing Shear Wave Estimation Through Directional and Kalman Filters for Noise Reduction

Sy Hiep Nguyen, Quang Hai Luong, Duc Nghia Tran,
Thi Thuong Vu, Trung Hoang Nguyen and Duc Tan Tran

July 25, 2023

Enhancing Shear Wave Estimation through Directional and Kalman Filters for Noise Reduction

Nguyen Sy Hiep[1], Luong Quang Hai[2], Tran Duc Nghia[3], Vu Thi Thuong[4], Hoang Trung Nguyen[5], Tran Duc Tan[6*]

[1]University of information and communication technology
Thai Nguyen, Vietnam

Nshiep@ictu.edu.vn

Le Quy Don Technical University, Hanoi, Vietnam

luonghai@mta.edu.vn

[3]Institute of Information Technology, Vietnam Academy of Science and Technology, Hanoi, Vietnam

nghiatd@ioit.ac.vn

[4]Phuong Dong University, Hanoi, Vietnam

thuongvt@dhpd.edu.vn

[5]General Department of Defense Industry, Hanoi, Vietnam

trungcnqp86@gmail.com

[6]Phenikaa University, Hanoi, Vietnam

tan.tranduc@phenikaa-uni.edu.vn

Abstract. The tissue elastography ultrasound technique has witnessed significant advancements in recent years. It is a non-invasive, cost-effective and highly reliable method. This approach estimates the elasticity and viscosity of diseased tissue by utilizing an ultrasonic Doppler probe to measure the velocity of shear waves. However, this technique faces challenges due to the presence of noise caused by reflected waves and random noise, which can impact the accuracy of the results. To address this issue. we employ a directional filter to eliminate reflection noise before using a Kalman filter to estimate elasticity and viscosity.

Keywords: Shear wave, reflection, ultrasonic, kalman filter, directional filter.

1 Introduction

Tissue elastography imaging has significantly contributed to early disease diagnosis in various organs, including the breast, thyroid gland, liver, and prostate gland. Modern ultrasound devices now offer the capability to generate elastographic images that provide valuable information about tissue properties

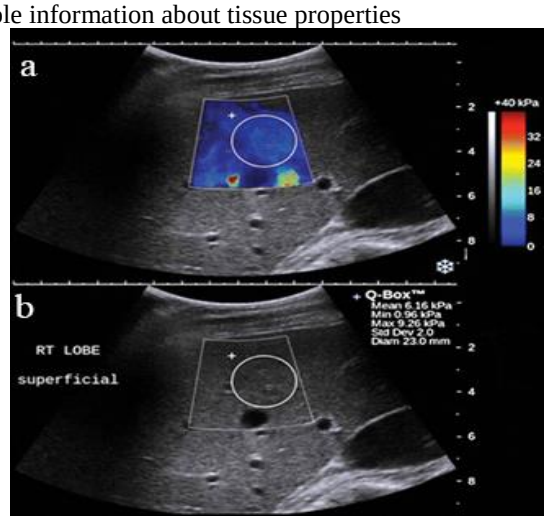

Fig. 1. (a) Elastography image showing high peritumoural stiffness (mean 40kPa) (b) B mode image [15].

In Fig.1(b), the gray-scale image represents the B-mode ultrasound. The B-mode image provides information about the structural characteristics of the tissue. While Fig.1(a), the image displays the elastography ultrasound. The color scale represents the stiffness of tissue, The range of dark blue to red indicates the ascending the stiffness of tissue. By analyzing the color patterns in the image, doctors can identify areas of tissue that are stiff and show signs of pathology.

1.1 Human tissue elasticity

To quantify tissue stiffness, a physical parameter known as Young's modulus is employed. This parameter is calculated by applying a uniform, external compression (or stress S) to diseased tissue, which generates a corresponding deformation (e) within the tissue. By measuring this deformation, the stiffness of the tissue can be evaluated and diagnosed.

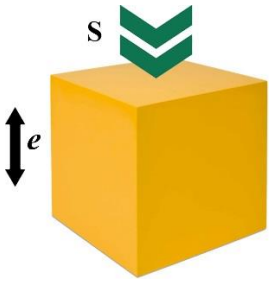

Fig. 2. Deformation of solid under an external stress.

$$E = \frac{s}{e} \tag{1}$$

where s is external stress, e is strain inside the tissue, E is Young Modulus.

Hard tissue is characterized by higher density compared to soft tissue, and diseased tissue typically exhibits greater stiffness than healthy tissue. For instance, the young modulus of breast adipose tissue ranges from 18 to 24 kPa, while fibrous tissue falls within the range of 96 to 244 kPa. Normal liver has a value of 0.4 to 6 kPa, whereas cirrhosis E demonstrates arange from 15 to 100 kPa. The density of tissues in the body is known to be approximately 1000 kg/m^3. While tissue density remains relatively constant, tissue elasticity can vary significantly depending on the pathological state. In terms of wave propagation, compression waves travel at a faster pace in tissue at approximately 1500 m/s, while shear waves propagate at a considerably slower speed of 1 to 10 m/s. There exists a correlation between tissue elasticity and the velocity of wave propagation [6].

$$E = \rho c^2 \tag{2}$$

Where ρ is density of tissues (1000kg/m^3), c is Shear wave propagation speed is external stress, e is strain inside the tissue, E is Young Modulus. By measuring the shear wave velocity and considering a tissue density of 1000 kg/m^3, it becomes possible to estimate the elasticity of the tissue [6], [7], [8].

1.2 Determination of elasticity and viscosity of tissues

In this paper, we employed a vibrating needle to generate deformation waves and measured their propagation velocity within the tissue environment. This allowed us to calculate the viscosity and elasticity of the examined tissue [1], [2]. However, during the propagation of the incident waves, they were influenced by reflections caused by the heterogeneity of the transmission medium and random noise. To address these challenges, we utilized directional filtering and Kalman filtering techniques to effectively eliminate noise and enhance the accuracy of our measurements [3],[4]. We calculated the velocity of the shear wave at a specific location indicated by the wave propagation equation [6], [9], [10].

Equation of the incoming wave

$$v_n(r) = \frac{1}{\sqrt{r - r_0}} A e^{-a(r-r_0)} \cos[\omega n \Delta t - k_s(r - r_0) - \phi] \quad (3)$$

The heterogeneity of the tissue causes the acoustic wave to undergo reflection at the boundary between two different environments. This phenomenon affects the accuracy of measuring the shear wave velocity.

The equation for the reflected wave is represented by equation (4)

$$v_n(r) = \frac{1}{\left(\sqrt{r_{f0} - r}_f\right)} \frac{A}{C} e^{-a(r-r_0)} \cos[-\omega n \Delta t + k_s(r_{f0} - r_f) - \phi] \quad (4)$$

Table 1. Parameters used in equations (3) and (4)

r	The spatial coordinate of the incoming wave.	ϕ	The Initial phase
r_0	The coordinates of the incoming wave's source	k_s	The wave number
r_f	The spatial coordinate of the reflected wave.	$\frac{A}{C}$	The amplitude of the reflected wave's source
r_{f0}	The coordinates of the reflected wave's source		
A	The amplitude of the incoming wave's source	ω	The angular frequency
Δt	The time step	α	The attenuation coefficient
n	The number of time step	v	The velocity

According to the Kelvin-Voigt model, the calculation of elasticity (E) is equivalent to determining the complex shear modulus [11], [12], [13].

$$\mu = \mu_1 - i\omega\eta \quad (5)$$

For accurate location analysis, it is important to determine the elasticity and viscosity of the medium at that specific location.

Viscosity and elasticity are calculated based on equations (6) and (7).

$$\eta = -\frac{2\rho\omega k_s \alpha}{(k_s{}^2 + \alpha^2)^2} \quad (6)$$

$$\mu_1 = \frac{\rho\omega^2(k_s{}^2 - \alpha^2)}{(k_s{}^2 + \alpha^2)^2} \tag{7}$$

Where μ is complex Shear Modulus, η is viscosity of the medium, μ_1 is tissue elasticity

2 Data processing flow

The received signal is a composite signal consisting of the incident wave, the reflected wave, and random noise. The noise needs to be eliminated to obtain a signal that closely resembles the incident wave. The data processing flow is illustrated in Fig.3 [9].

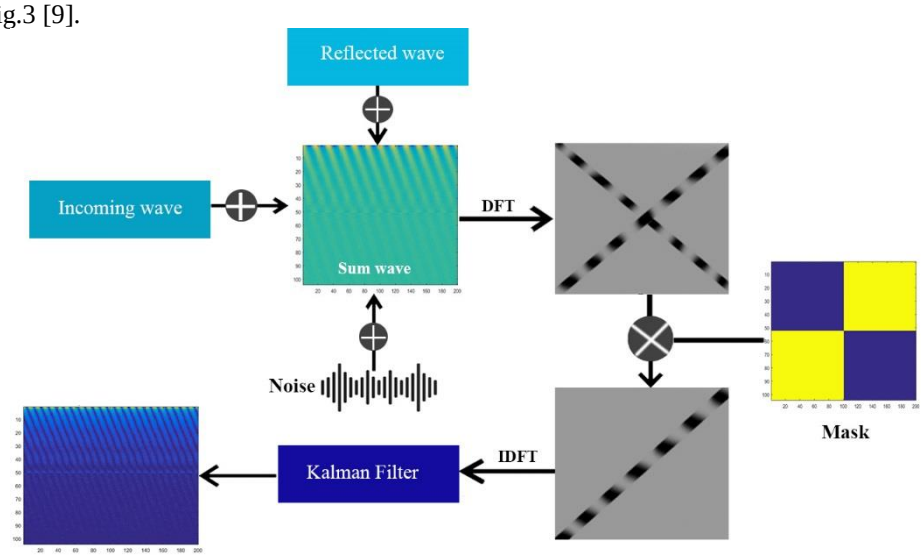

Fig. 3. Data processing flow.

In Fig.3, it illustrates the data processing flow using a directional filter and Kalman filter to remove noise from the acquired signals. This noise includes reflections from the reflected waves and random noise added to the incident wave signal. The composite signal undergoes Fourier transformation and is multiplied by the directional filter mask. Subsequently, the signal is inverse Fourier transformed and passes through the Kalman filter before yielding the final velocity signal. This velocity signal is then used to generate graphs representing tissue viscosity and elasticity.

Directional Filter

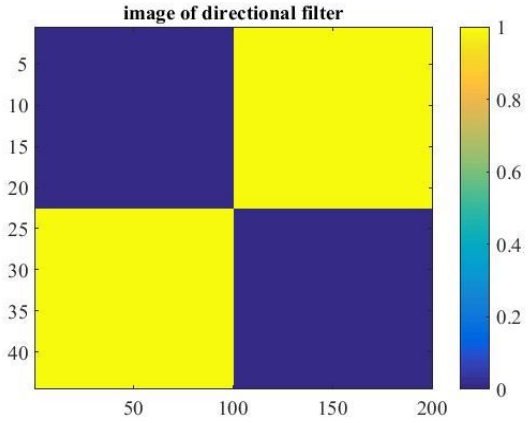

Fig. 4. Image of directional filter mask

The input signal is transformed using the Fourier transform, and then it is multiplied by the mask matrix shown in Fig.4. This matrix determines which signals are preserved and which are discarded, with a value of 1 representing signals to be transmitted (yellow) and a value of 0 representing signals to be filtered out (dark blue). Finally, the processed signal is converted back to its original form [14].

Kalman filter

Specifically in this paper, the Kalman filter is utilized to estimate the propagation velocity of shear waves in the tissue. The filter considers the noisy measurements of wave propagation and combines them with previous estimates to obtain an improved estimation of velocity. Through the use of the Kalman filter, the authors aim to mitigate the impact of random noise and enhance the accuracy of wave velocity estimation in the tissue.

3 System setup and results

3.1 System setup

In this paper, we utilize MATLAB for simulation purposes, and the input data is obtained from the values provided in Table

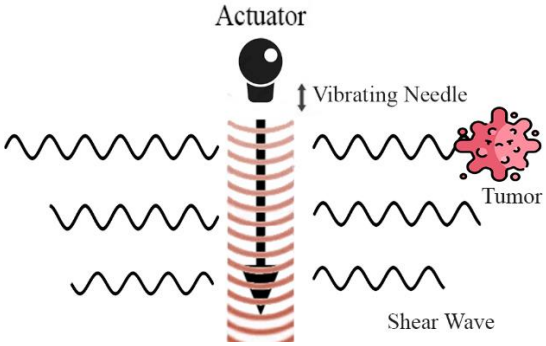

Fig. 5. Vibrating needle generate shear wave.

Table 2. The information is presented in the following table.

Frequency	100Hz
Amplitude of incident wave	0.003
Amplitude of reflected wave	0.0003
Normal tissue viscosity	650k Pas
Normal tissue elasticity	0.1kPa
Elasticity of diseased tissue	800kPa
Viscosity of diseased tissue	0.2kPas
Density	1000kg/m^3

3.2 Results

We assess the impact of filters by comparing the outcomes before and after its application.

Before using directional filter and Kalman filter

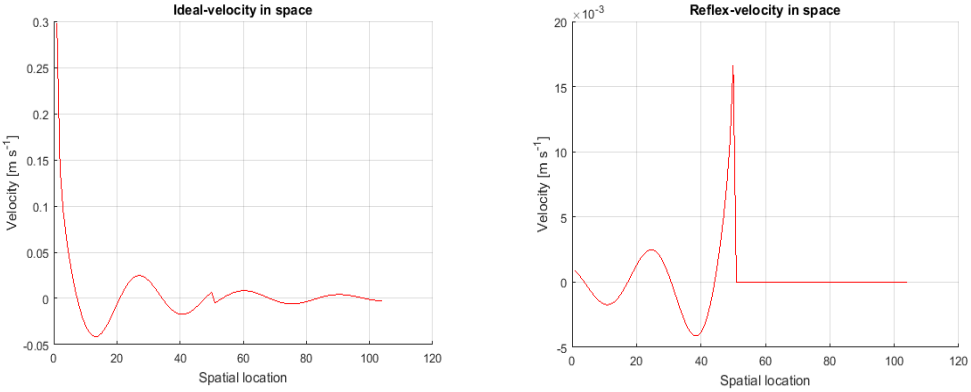

Fig. 6. (a) Incomming wave. (b) Reflected wave.

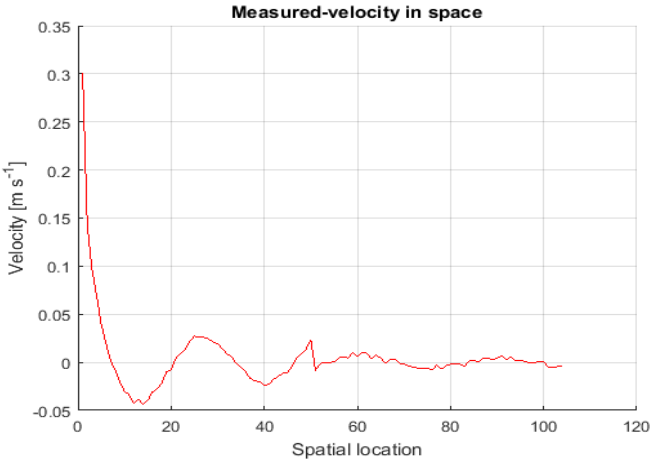

Fig. 7. Mix wave

Image Fig.6 (a) represents the graph of the incident wave, while image Fig.6 (b) represents the graph of the reflected wave. The reason for the attenuation and presence of this reflected wave in the incident wave is due to the presence of diseased tissue towards the right side of position 50, while healthy tissue is present towards the left side. The viscosity and elasticity values for the respective tissues are provided in Table R. Image Fig.7 depicts the composite wave graph, illustrating the influence of the reflected wave on the composite wave.

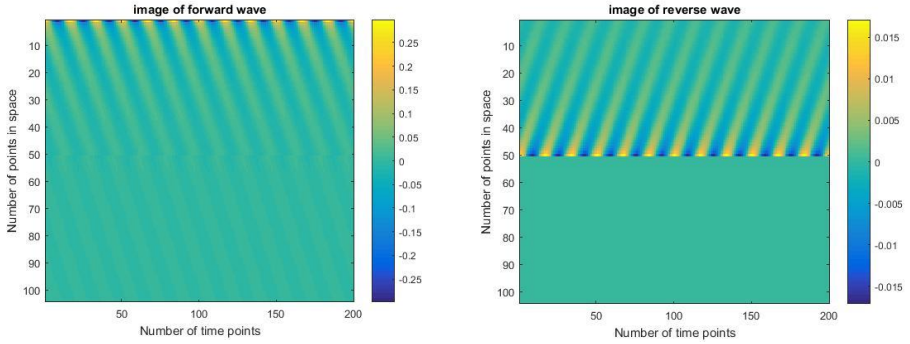

Fig. 8. (a) Image of incident wave. (b) Image of reflected wave.

The color represents the amplitude of the propagating wave, with a maximum value of 0.3 and a minimum value of -0.3. Observing graph Fig.8 (a), we notice that its value is highest at the source and diminishes as it moves away from the source. Particularly, there is a significant reduction in energy at position number 50. This is due to the interaction of the sound wave with the boundary between healthy and diseased tissue, causing partial reflection. In graph Fig.8 (b), we observe the opposite pattern, where the energy of the reflected wave reaches its peak at position number 50 and gradually attenuates towards the source.

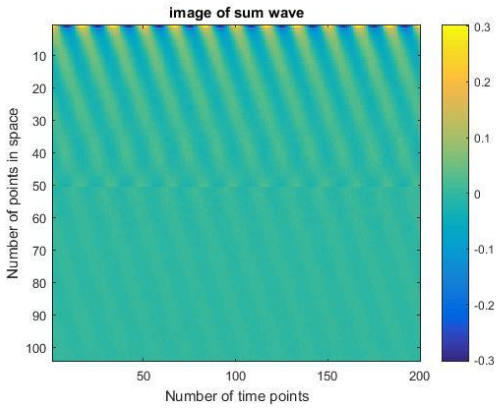

Fig. 9. Image of sum wave before using filters.

In image Fig.9, we observe the composite wave formed by the incident wave and the reflected wave. It is evident that at position 50, there is significant dynamic noise present. This indicates that the reflected wave has an influence on the incident wave, causing interference. To obtain accurate signals, it is crucial to minimize the impact of the reflected wave on the incident wave as much as possible.

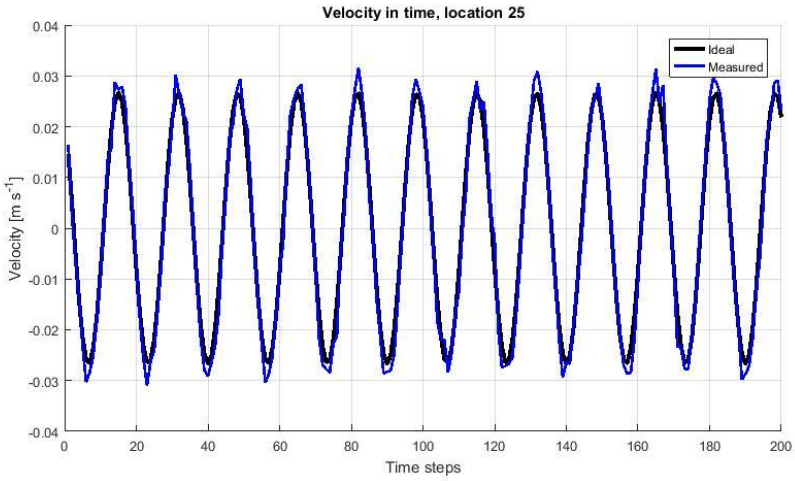

Fig. 10. The mix wave before using filters.

The velocity at a specific point at position 25 fluctuates over time and follows a pattern as shown in Figure.10. Figure.11 represents the graph of the synthesized wave before using filters, with the black line indicating the ideal graph and the green line representing the measured signal.

After using directional filter and Kalman filter

The application of the directional filter results in the removal of data propagating from right to left, retaining only the information pertaining to the incoming wave.

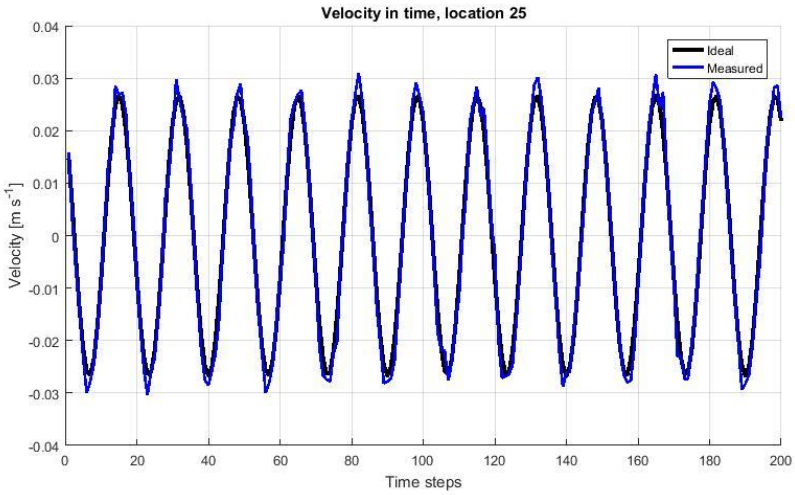

Fig. 11. The mix wave after using filters.

Based on Figures 10 and 11, it can be observed that after passing through filters, the measured signal in Figure 12 closely resembles the ideal graph more than in Figure 10.

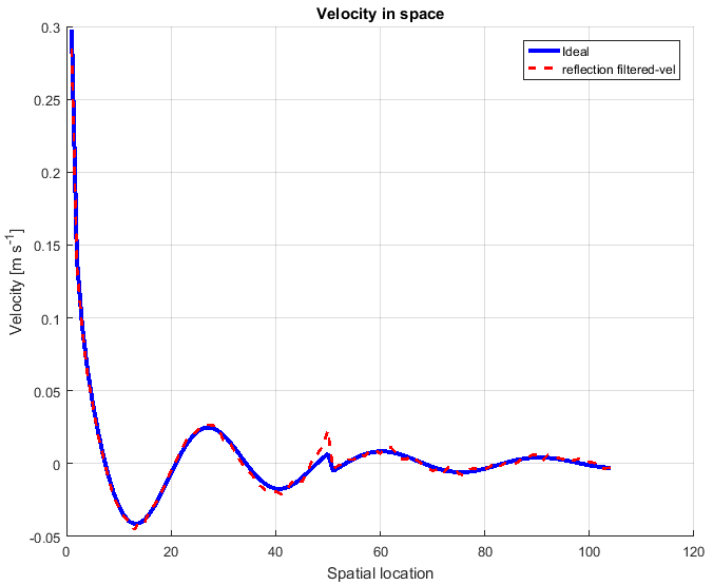

Fig. 12. Velocity in space.

In Figure.12, the blue line represents the ideal velocity graph in space, while the red line represents the velocity of the synthesized wave in space after passing through filters, which helps reduce the impact of reflected noise. The red graph closely aligns with the ideal blue graph.

The amplitude of both the blue and red graphs reaches its maximum value at the source point (0) and decreases as they move away from the source. Both graphs exhibit a pronounced response at position 50, which represents the boundary between healthy and diseased tissue based on the input data of the problem. Based on the obtained velocity data. We will extract information about the characteristics of the diseased tissue, specifically the values of elasticity and viscosity.

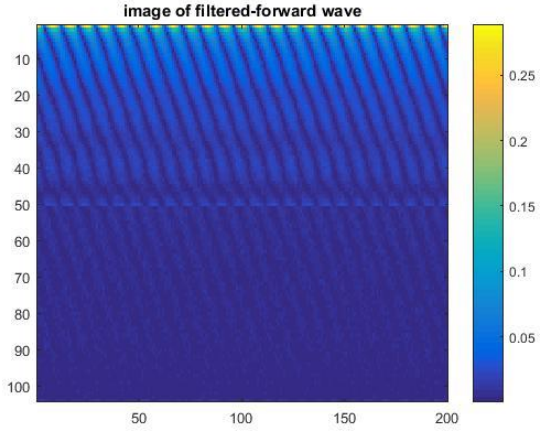

Fig. 13. Image of forward wave after using filters.

The image of the transmitted wave is filtered after passing through filters. The color scale on the right represents the amplitude of the shear wave, with the maximum amplitude located at the source and decreasing as the wave moves away from the signal source

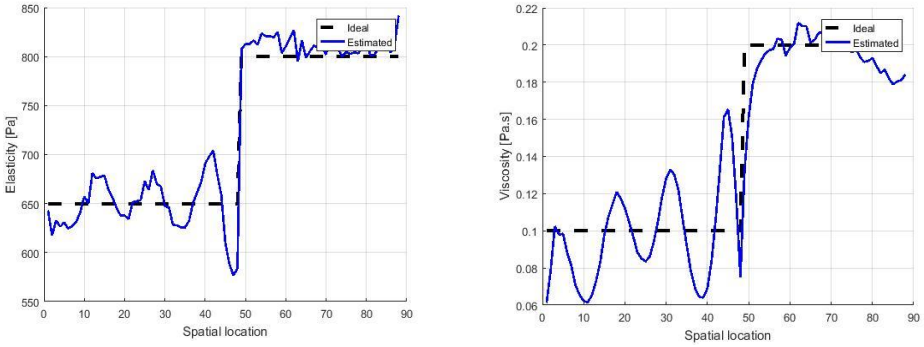

Fig. 14. (a) The elasticity of tissue (b) The viscosity of tissue

After calculating the velocity of the sound wave traveling from the starting point to point 90, we can reconstruct the elasticity and viscosity of the tissue. In Fig.14 (a) and Fig.14 (b), the dashed lines represent the ideal conditions of elasticity and viscosity without any noise, while the blue line represents the measured signal with noise and filtering. Both the blue lines and dashed lines exhibit a strong response at position 50, which represents the boundary between healthy and diseased tissue.

By determining the propagation velocity of the sound wave, we can accurately determine the viscosity and elasticity of the tissue. This valuable information aids in diagnosing abnormal tissue conditions. Furthermore, in this paper, directional filter and Kalman filter are employed to eliminate the influence of noise caused by reflected waves, thereby increasing diagnostic accuracy.

References

1. Bercoff J, Tanter M, Fink M. Supersonic, "Shear imaging: a new technique for soft tissue elasticity mapping." IEEE Transactions on Ultrasonics, Ferroelectrics, and Frequency Control, 2014.
2. Sigrist RMS, Liau J, Kaffas AE, Chammas MC, Willmann JK, "Ultrasound elastography: review of techniques and clinical applications," Theranostics 2017.
3. Pengfei Song1,2, Armando Manduca1, Heng Zhao1, Matthew W. Urban1, James F.Greenleaf, Shigao Chen, "Fast Shear Compounding Using Robust Two-dimensional Shear Wave Speed Calculation and Multi-directional Filtering." Ultrasound Med Biol. 2014 June, 2014.
4. Thomas defeux, Jean-luc Gennisson, Jeremy bercoff, and Mickael Tanter "On the Effects of Reflected Waves in Transient Shear Wave Elastography." IEEE TransacTIons on UlTrasonIcs, FErroElEcTrIcs, and FrEqUEncy conTrol, vol. 58, no. 10 , 2011.
5. Andrew Evans, Patsy Whelehan, Kim Thomson, Katrin Brauer, L Jordan, Colin Purdie, D McLean, Lee Baker, Sarah Vinnicombe, Alastair M Thompson,"Differentiating benign from malignant solid breast masses: Value of shear wave elastography according to lesion stiffness combined with greyscale ultrasound according to BI-RADS classification" British Journal of Cancer · June 2012, June 2012.
6. Quang-Hai Luong, Manh-Cuong Nguyen, Tan Tran-Duc, "Complex shear modulus estimation using extended kalman filter." Tạp chí khoa học& kỹ thuật số179, 2016.
7. Carlson, L.C.; Feltovich, H.; Palmeri, M.L.; Dahl, J.J.; Munoz del Rio, A.; Hall, T.J. "Estimation of shear wave speed in the human uterine cervix." Ultrasound Obstet. Gynecol. 2014, 43, 452–458, 2014.
8. Dalong Liu Emad S. Ebbini Viscoelastic Property Measurement in Thin Tissue Constructs Using Ultrasound IEEE Transactions on Ultrasonics, Ferroelectrics, and Frequency Control. 2008 February, 2008.
9. Nguyen Thi Hao, Tran Thuy-Nga, Vu Dinh-Long, Tran Duc-Tan, Nguyen Linh-Trung, "2D Shear Wave Imaging Using Maximum Likelihood Ensemble Filter." International Conference on Green and Human Information Technology (ICGHIT 2013), 2013.
10. Walker WF, Fernandez FJ, Negron LA, "A method for imaging viscoelastic parameters with acoustic radiation force Phys." Med. Biol 2000;vol. 45:1437–1447, 2000.
11. H. Yuan, B.B. Guzina, S. Chen, R.R. Kinnickb and M. Fatemi "Estimation of the complex shear modulus in tissue-mimicking materials from optical vibrometry measurements." Inverse Problems in Science and Engineering Vol. 00, No. 00, March 2011.

12. Antonio Callejas, Antonio Gomez, Inas H. Faris, Juan Melchor and Guillermo Rus," Kelvin–Voigt Parameters Reconstruction of Cervical Tissue-Mimicking Phantoms Using Torsional Wave Elastography." Sensors 2019, 19, 3281; doi:10.3390/s19153281, 2019.
13. Tran Quang Huy, Pham Thi Thu Ha, Tran Binh Duong,Nguyen Quang Vinh, Nguyen Thi Hoang Yen, Tran Duc Tan, "2D Shear Wave Imaging in Gaussian Noiseand Reflection Media." VNU Journal of Science: Mathematics – Physics, Vol. 37, No. 4, 2021.
14. Shaozhen song, Nhan Minh Le, Zhihong huang "Quantitative shear-wave optical coherence elastography with a programmable phased array ultrasound as the wave source." Article in Optics Letters · October 2015 2015.
15. Anthony E. Samir , Manish Dhyani, Abhinav Vij, Atul K. Bhan, Elkan F. Halpern, Jorge Méndez-Navarro, Kathleen E. Corey, Raymond T. Chung "Shear-Wave Elastography for the Estimation of Liver Fibrosis in Chronic Liver Disease: Determining Accuracy and Ideal Site for Measurement". RSNA Journals, publish online Nov 13 2014.